PHOTOCATALYTIC EFFICIENCY OF LANTHANIDE-DOPED ZINC OXIDE FOR DEGRADATION OF METHYLENE BLUE DYE

MAISHARA SYAZRINNI ROOSHDE[1], WAN RAFIZAH WAN ABDULLAH[*,1], NORADHIHA FARAHIN IBRAHIM[1], MOHD SABRI MOHD GHAZALI[2] AND WAN MOHD NORSANI WAN NIK[1]

[1]*School of Ocean Engineering, 2School of Fundamental Science, Universiti Malaysia Terengganu, 21030 Kuala Nerus, Terengganu, Malaysia.*

**Corresponding author: wanrafizah@umt.edu.my*

Abstract: Photocatalytic treatment of dyeing wastewater using zinc oxide (ZnO) is a promising approach due to its economic viability, energy efficiency and environmental friendliness. In order to improve the environmental sustainability of existing photocatalysis based treatment technology, doping technique is performed on pristine semiconductor material to produce highly efficient photocatalyst. In this study, the potential use of lanthanide (Ce, Er, La and Pr) -doped ZnO as photocatalyst powder have been investigated for the degradation of methylene blue (MB) dye solution. Powder form photocatalyst was successfully prepared by doping ZnO at 1 mol % of lanthanides through combination of citrate gel and solid state means. The synthesized lanthanide-doped ZnO photocatalyst powder was characterised by using XRD, SEM and EDS. The photocatalyst of various loads (0.5 - 2.0 g/L) was used to induce photodegradation of 10 mg/L MB dye solution under UV-light illumination up to 180 minutes. The treated MB solution was characterized by using UV-Visible Spectrophotometer. The findings showed that the photocatalytic efficiency increased with the increase in catalyst loadings. The highest photocatalytic efficiency (94.32%) was achieved by treatment using 2.0 g/L of 1 mol % Er doped ZnO. The list of photocatalysts in the order of decreasing photocatalytic efficiency is Er doped ZnO (94.32%) > Ce doped ZnO (93.81%) > La doped ZnO (72.16%) > and Pr doped ZnO (67.67%). The Er and Ce doped ZnO based photocatalysts have proven efficiency to induce oxidation of organic dye in wastewater and they are indeed promising candidates for future solar-driven photocatalyst.

Keywords: Photocatalyst, Lanthanide-doped ZnO, Methylene Blue, Photocatalytic degradation, sustainable treatment.

Introduction

Water pollution is becoming a growing concern and worldwide environmental problem. Discharge of effluent from dyeing industry is one of the biggest contributors to water pollution. Dyes are really hard to be decolourised due to its high chroma-intensity and difficulty to biodegrade when being discharged into the water stream (Yi *et al.,* 2008; Fan *et al.,* 2009; Zhuang *et al.,* 2009). Dyes are also hazardous to the environment for having large number of contaminants and chemicals including benzidine and metals (Arafat, 2007). Therefore, numerous methods have been developed to treat dyes in wastewater. By that, removing organic pollutants via photocatalytic methods have gained much attention for its outstanding advantages including high efficiency and energy economy. Heterogenous photocatalysis are extensively being used due to its minimal production of waste, non-toxicity, high efficiency and claimed as sustainable wastewater treatment technology (Josephine *et al.,* 2015; El Saliby *et al.,* 2016).

Over decade, ZnO has been considered as one of the promising photocatalysts due to its high chemical stability, high photostability, non-toxicity, low cost and high efficiency in photocatalysis (Kołodziejczak-Radzimska & Jesionowski, 2014). Nevertheless, current findings suggest that efficiency of ZnO can be increased by doping it with rare earth materials (Alam *et al.,* 2018; Kumar *et al.,* 2018; Cerrato *et al.,* 2018). This technique has been approached and it is proven that the photocatalytic efficiency

of ZnO increases through doping with some elements including Cerium, Ce (Kumar *et al.,* 2015) and Europium, Eu (Phuruangrat *et al.,* 2014), Dysprosium, Dy (Kumar *et al.,* 2018). The effect of using lanthanides as dopant in ZnO based photocatalysts is somehow limited compared to transition metal dopants. Hence, this study presents the investigation of the photocatalytic properties of lanthanide-doped ZnO for degradation of methylene blue (MB) dye under UV light irradiation.

Materials and Methods

Material

ZnO doped with a series of lanthanides namely cerium (Ce), erbium (Er), lanthanum (La), and praseodymium (Pr) were synthesized and characterized as photocatalyst of interest. The raw materials required for the photocatalyst powder preparation were supplied by Sigma Aldrich. They are commercial grade ZnO, erbium (III) acetate hydrate ($(CH_3CO_2)_3Er.XH_2O$) lanthanum (III) acetate hydrate ($La(CH_3CO_2)3.XH_2O$) and cerium (III) nitrate hexahydrate ($Ce(NO_3)_3.6H_2O$. Praseodymium (III) acetate hydrate ($Pr(CH_2COOH)_3.xH_2O$) was supplied by Alfa Aesar and citric acid anhydrous ($C_6H_8O_7$) by Fluka, was employed as a chelating agent. Methylene blue trihydrate ($C_{16}H_{18}C1N_3S.3H_2O$) (Duksan Pure Chemical Company) was extensively used as organic dye representative.

Preparation of Doped Zno Photocatalyst Powder

Lanthanide-doped ZnO powder was obtained through citrate gel technique. The right amount of stoichiometric lanthanide (Ce, Er, La and Pr) nitrate or acetate salt powder was separately added into aqueous solution of citric acid and gradually added ZnO powder into the beaker. The mixture was magnetically stirred at 80-100°C for 4 h on a hot plate and was further dried at 110°C for 19 h before sending for calcination at 500°C for 4 h followed by sintering in a box furnace at 1200°C for 5 h. Finally, the synthesized powder was sieved to reduce the particle size to less than 63 μm.

Characterizations of Precursor Photocatalytic Powder

Phase analysis was carried out by using an X-ray Diffractometer machine (Rigaku Miniflex II Model PW1710) with Cu Kα radiation having a wavelength, λ of 1.54. The morphology and elemental distribution on the prepared samples were carried out by using Hitachi Tabletop Microscope TM3030Plus. The concentration of MB dye during photodegradation treatment was determined by using Shimadzu UV-1800 spectrophotometer.

Evaluation of Photocatalytic Performance

Photocatalytic performance of the lanthanide (i.e Er, Ce, La, Pr)-doped ZnO was evaluated based on photodegradation rate of 10 mg/L of methylene blue (MB) dye solution under UV light (λ=254 nm). For each set of experiment, 0.5 to 2.0 g/L of photocatalyst powder was loaded into 10 mg/L of MB dye solution and it was vigorously stirred for 30 minutes in the dark to equilibrate the adsorption of dye molecules on the catalyst particles (Kumar *et al.,* 2008). UV light irradiation was prolonged up to 180 minutes. Solution sample withdrawal was performed at 15-minute intervals and sent for UV-vis analysis. The residual concentration of MB was measured by monitoring the max absorption peak at the wavelength of 665 nm using UV-Vis spectrophotometer. Photocatalytic efficiency, R value was calculated based on Equation 1.

$$Photocatalytic\ effieciency, R(\%) = \frac{(C_o - C_t)}{C_o} \times 100 \qquad (1)$$

where C_o is the initial concentration of dye (mg/L) and C_t is the concentration of dye at irradiation time, t (mg/L).

The photocatalytic degradation of MB was studied according to Langmuir Hinshelwood model. The pseudo-first order rate constant,

k was evaluated from the slope of the – (ln (C_t/C_o) = kt. The rate expression of MB dye concentration is given by Equation 2.

$$-\left(ln\frac{C_t}{C_o}\right) = kt \quad (2)$$

where k is the pseudo-first order rate constant; C_o is the equilibrium concentration of dye, and C_t is the concentration at time(min). The higher the k value, the more rapid the photodegradation reaction will take place.

Results and Discussion

Characteristics of Ce Doped Zno Powder

Figure 1 shows the XRD patterns of the prepared samples. Phase analysis revealed that calcination and sintering processes successfully transforming the precursors into intended Er, La, Pr and Ce doped ZnO. As compared to the diffraction peaks for prestine ZnO (Fig. 1a), additional peaks marked as (♦), (♣), (○) and (▲) in Figure 1b - e indicate the presence of predetermined dopant in oxide form within respective sample. Diffraction peaks of hexagonal wurtzite structure ZnO (PDF card no. 80-75) were detected along with the dopants including cerium oxide (CeO_2) with PDF card no 65-2975, erbium oxide (Er_2O_3) with PDF card no 77-459, lanthanum oxide (La_2O_3) with PDF card no 89-4016 and praseodymium oxide (Pr_6O_{11}) with PDF Card no 42-1121, respectively. No spinel phases were detected. Full conversion of dopant precursor to polycrystalline oxide phase through calcination and sintering processes is crucial to ensure its doping impact on photoactivity of ZnO host.

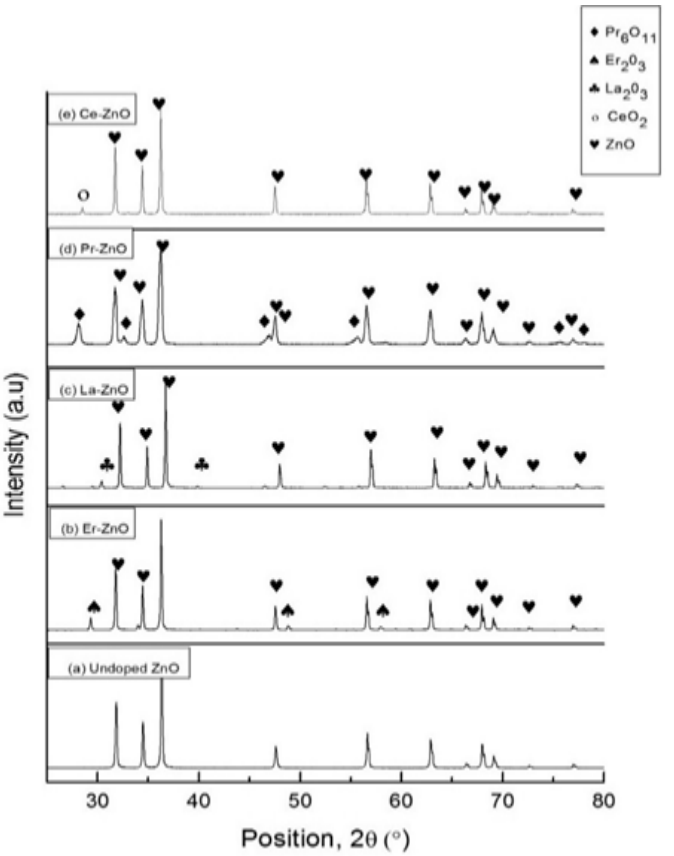

Figure 1: XRD patterns of (a) undoped ZnO, (b) Er doped ZnO, (c) La doped ZnO, (d) Pr doped ZnO and (e) Ce doped ZnO

The morphology and particle size distribution of doped ZnO were evaluated under tabletop microscope at 10,000 times magnifications. Figure 2 depicts the backscattered electron images of ZnO doped with 1 mol% of either Er, Ce, La or Pr. The addition of different doping elements slightly altered the size and uniformity of the ZnO grains. ZnO doped with 1 mol% Er comprised clusters of very fine ZnO grains. Er_2O_3 nanoparticles resulted from citrate gel preparation technique evenly distributed within the grains. Introduction of 1 mol% of other elements such as Ce, La and Pr produced agglomerated ZnO particles. The ZnO grains have coarsened after sintering process and diffused with neighboring grains. Agglomeration effects are the most obvious in Pr doped ZnO. Particle size distribution and the size of clusters determined the total contact surface area reachable by photon, thus controlled the photoactivity of photocatalyst upon illumination of light.

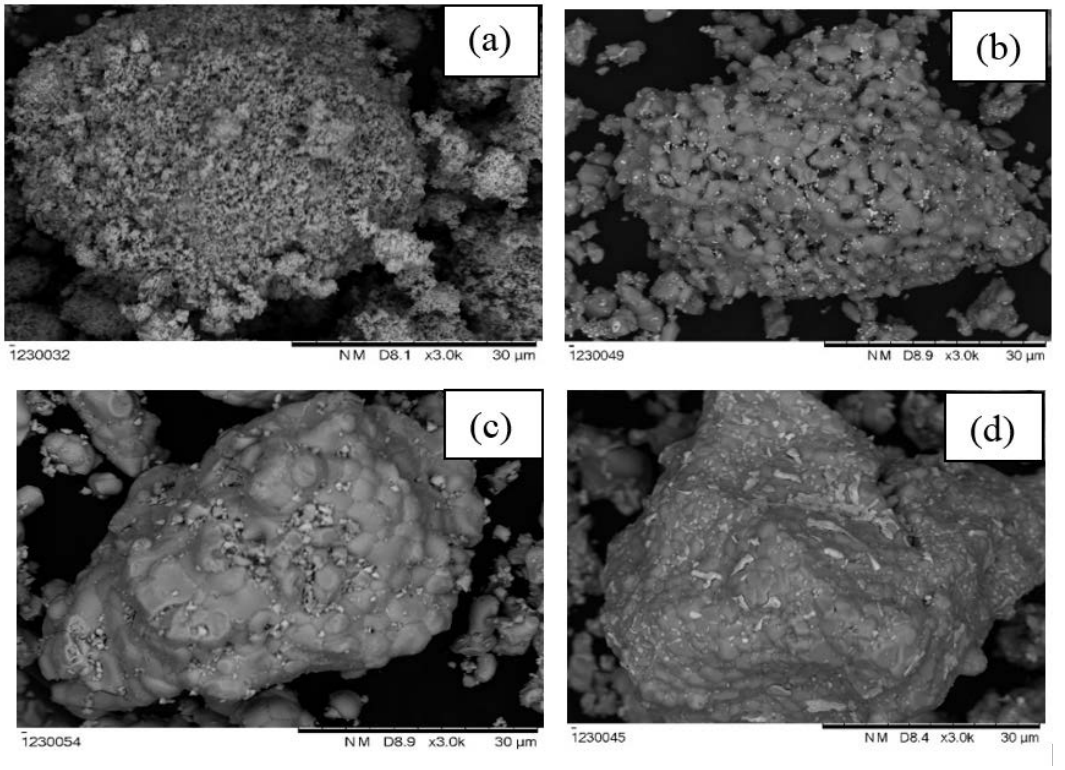

Figure 2: Backscattered electron images of 1 mol % (a) Er doped ZnO, (b) Ce doped ZnO, (c) La doped ZnO and (d) Pr doped ZnO.

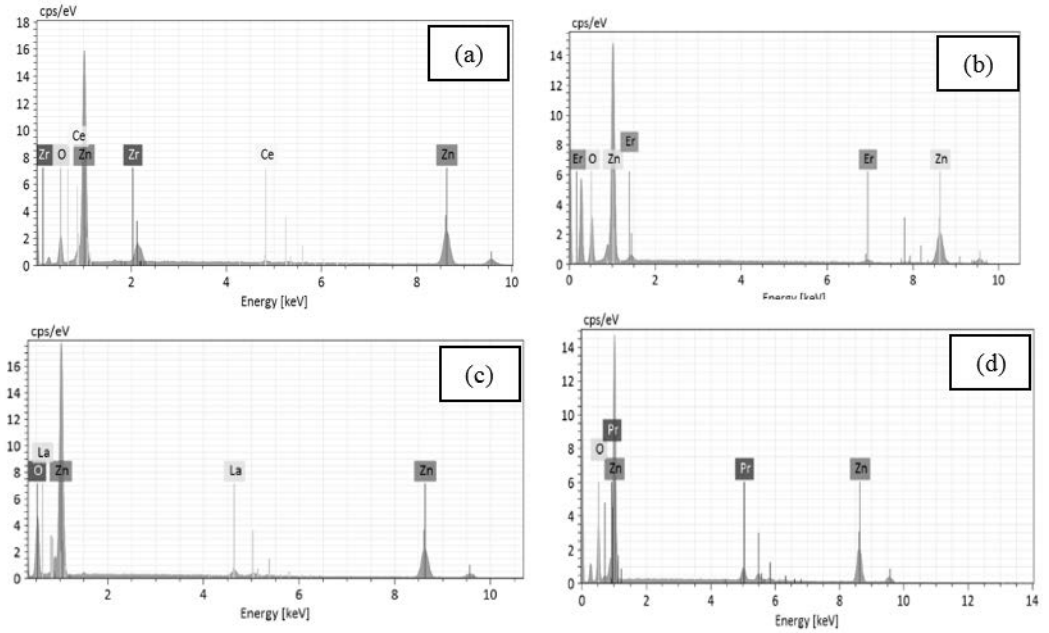

Figure 3: EDS spectra for 1 mol % of (a) Ce doped ZnO (b) Er doped ZnO (c) La doped ZnO and (d) Pr doped ZnO.

Dispersive X-Ray Spectroscopy (EDS) was conducted in order to analyze and confirm the elemental distribution in each types of dopants. Figure 3 shows the corresponding EDS mapping to images in Figure 2. Er, Ce, La and Pr elements were respectively detected and reflected in the EDS spectrum of its doped ZnO powder. Doping element was distributed at the exterior of ZnO grains or preferentially segregated as cluster of oxide precipitates in between ZnO grains. No other elements and peaks were detected in the spectrum.

Photodegradation Performance of Lanthanide-Doped Zno

Photocatalytic efficiency of the doped ZnO powder was evaluated based on photodegradation process of MB dye solution. The findings from this work showed that the synthesized powder exhibited satisfactory photocatalytic reactivity particularly under energetic UV light. Through photocatalytic mechanism, the presence of Er, Ce, La and Pr doped ZnO capable of inducing hydroxyl radicals that responsible for breaking the dyes molecules into less complex compound.

Variation in photocatalytic efficiency was observed due to incorporation of different doping species and the amount of catalyst loading used during photodegradation test. Figure 4 depicts the UV-Vis spectra of MB solution after photodegradation process for 180 minutes in the presence of various lanthanide-doped ZnO and catalyst loadings. Figure 5 shows the photocatalytic efficiency of lanthanide-doped ZnO as a function of UV irradiation time. All results are summarized in Table 1.

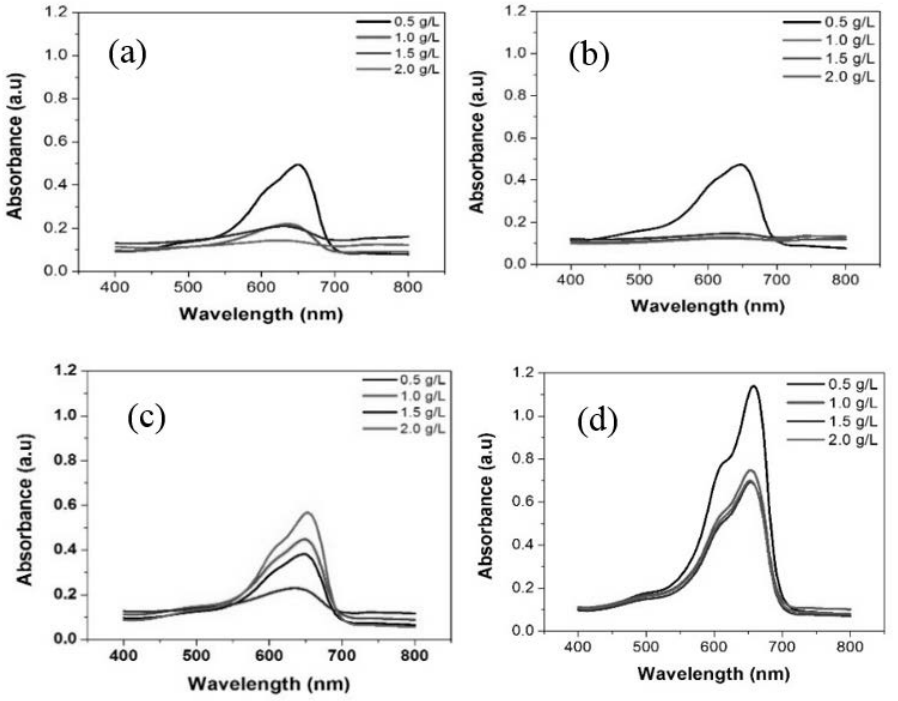

Figure 4: UV Vis spectra of MB dye solution after treatment with a) 1 mol % Er doped ZnO (b) 1 mol % Ce doped ZnO (c) 1 mol % La doped ZnO and (d) 1 mol % Pr doped ZnO photocatalysts

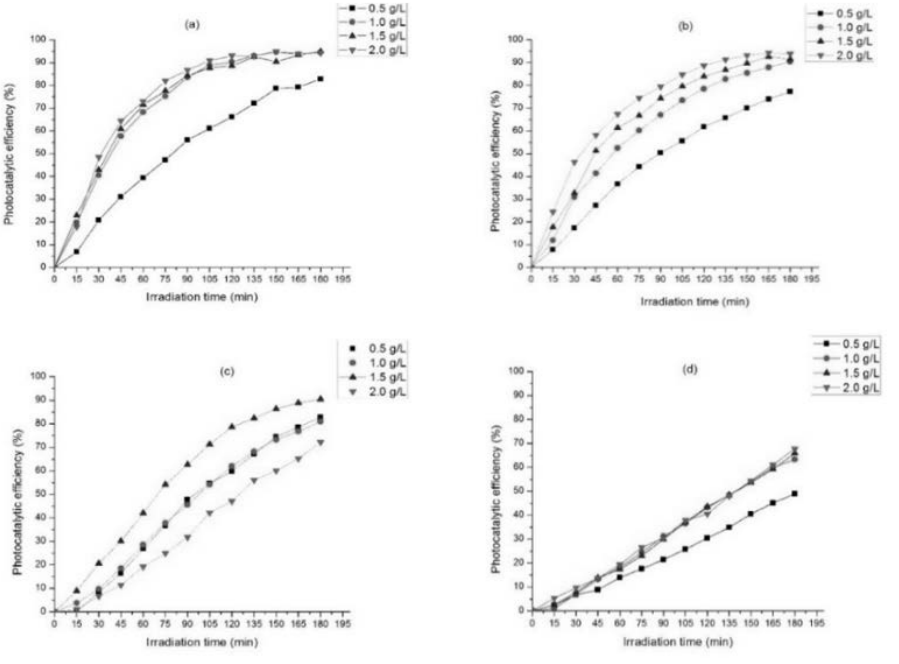

Figure 5: Variation in photocatalytic efficiency of a) 1 mol % Ce doped ZnO (b) 1 mol % Er doped ZnO (c) 1 mol % La doped ZnO and (d) 1 mol % Pr doped ZnO.

Table 1: Photocatalytic performance of 1 mol% lanthanides doped ZnO photocatalyst under UV light irradiation.

Dopant	Loading (g/L)	Photocatalytic efficiency, R (%)	Rate constant (min^{-1})
Er	0.5	82.77	0.0094
	1.0	94.45	0.0148
	1.5	94.86	0.0151
	2.0	94.32	0.0148
Ce	0.5	77.20	0.0078
	1.0	90.40	0.0123
	1.5	91.47	0.0126
	2.0	93.81	0.0139
La	0.5	82.76	0.0097
	1.0	80.95	0.0090
	1.5	90.38	0.0125
	2.0	72.16	0.0070
Pr	0.5	48.94	0.0036
	1.0	63.32	0.0058
	1.5	65.83	0.0058
	2.0	67.67	0.0060

The strongest photoreactivity was exhibited by ZnO photocatalyst doped with 1 mol% Er. This is based on the photocatalytic efficiency value and the rapidness of reaction or the high k value compared to the rest, followed by ZnO doped with equal molar concentration of Ce, La and finally Pr. General trend indicated that the photocatalytic efficiency increases with increasing loading of photocatalyst. This finding is predictable as the increases of loading provided more catalytic sites and improved photon absorption capacity. The highest photocatalytic efficiency (94.32%) was achieved by using 2.0 g/L of Er doped ZnO, whilst the lowest (48.94 %) was exhibited by 0.5 g/L of Pr doped ZnO. Exceeding the ZnO loading beyond 2.0 g/L may lead to a decreases in efficiency. Previous works by Chakrabarti & Dutta, (2004) and Sakthtivel *et al.* (2003) suggested that the removal efficiency of dyes by ZnO photocatalyst will decrease above its optimum loading as the excessive content of catalyst will increase turbidity and prevents the penetration of UV light, resulting lower photocatalytic performance (Sun *et al.,* 2008).

The performance of lanthanide-doped ZnO was attributed to its microstructure and electronic properties. Figure 2 showed the existence of very fine ZnO grains in Er doped ZnO powder contributed to larger catalytic surface area on photocatalyst to induce more rapid photodegradation process. In contrast, coarsening of ZnO grains and formation of agglomerated grains as observed in Ce, La and Pr doped ZnO reduced the effective catalytic surface area on photocatalysts. As a result, lower photoreactivity was observed even at similar loading value. Besides, the presence of different doping elements caused modification on its optical band gap energy. It was estimated that the optical band gap for Er_2O_3 doped ZnO is 3.2eV (John & Rajakumari, 2002), CeO_2 doped ZnO is 3.32eV (Varughese *et al.,* 2015), La_2O_3 doped ZnO is 3.37eV (Anandan *et al.,* 2007) and Pr_6O_{11} doped ZnO is 5.9 eV (Mbule, 2009). As band gap increased, the photocatalyst powder tend to covers only short range of the visible light spectrum and decreases the number of absorbed photon resulting in lower photocatalytic efficiency.

Conclusion

Lanthanide-doped ZnO photocatalyst powder were successfully prepared via modified citrate gel and solid state methods. The morphological and elemental analysis of the precursor powder were performed through XRD, SEM, and EDS techniques. The XRD patterns revealed that the photocatalyst powder contained hexagonal wurtzite structured ZnO and traces of lanthanide oxides. EDS analyses confirmed that the presence of dopants in the powder. The photocatalytic efficiency of lanthanide-doped ZnO is dependent on photocatalyst loading. Within the catalyst loading range of 0.5 to 2.0 g/L, the photocatalytic efficiency of doped ZnO increased with increasing amount of catalyst loading. Er doped ZnO powder exhibited the highest photocatalytic efficiency (94.32% by 2 g/L) compared to Ce, La and Pr doped ZnO. In addition, the findings suggest that both Er and Ce doped ZnO is highly efficient photocatalysts and they are indeed promising candidates for future solar-driven photocatalyst.

Acknowledgements

The authors thank the Ministry of Higher Education of Malaysia through Fundamental Research Grant Scheme (FRGS 59436) and Universiti Malaysia Terengganu for providing conducive facilities throughout this research. The authors declare that there is no conflict of interest.

References

Alam, U., Khan, A., Ali, D., Bahnemann, D. & Muneer, M. (2018). Comparative photocatalytic activity of sol–gel derived rare earth metal (La, Nd, Sm and Dy)-doped ZnO photocatalysts for degradation of dyes. *RSC Advances,* 8(31): 17582-17594.

Anandan, S., Vinu, A., Lovely, K. S., Gokulakrishnan, N., Srinivasu, P., Mori, T., Murugesan, V., Sivamurugan, V. & Ariga, K. (2007). Photocatalytic activity of La-doped ZnO for the degradation of monocrotophos in aqueous suspension. *Journal of Molecular Catalysis A: Chemical,* 266(1): 149-157.

Arafat, H. A. (2007). Simple physical treatment for the reuse of wastewater from textile industry in the Middle East. *Journal of Environmental Engineering and Science,* 6(1): 115-122.

Cerrato, E., Gionco, C., Berruti, I., Sordello, F., Calza, P., & Paganini, M. C. (2018). Rare earth ions doped ZnO: Synthesis, characterization and preliminary photoactivity assessment. *Journal of Solid State Chemistry,* 264: 42-47.

Chakrabarti, S. & Dutta, B. K. (2004). Photocatalytic degradation of model textile dyes in wastewater using ZnO as semiconductor catalyst. *Journal of Hazardous Materials,* 112(3): 269-278.

El-Saliby, I., McDonagh, A., Erdei, L. & Shon, H. K. (2016). Water reclamation by heterogeneous photocatalysis over titanium dioxide. *Green Technologies for Sustainable Water Management.*

Fan, J., Guo, Y., Wang, J. & Fan, M. (2009). Rapid decolorization of azo dye methyl orange in aqueous solution by nanoscale zerovalent iron particles. *Journal of Hazardous Materials,* 166(2): 904-910.

John, R. & Rajakumari, R. (2012). Synthesis and characterization of rare earth ion doped nano ZnO. *Nano-Micro Letters,* 4(2): 65-72.

Josephine, G. S., Ramachandran, S. & Sivasamy, A. (2015). Nanocrystalline ZnO doped lanthanide oxide: an efficient photocatalyst for the degradation of malachite green dye under visible light irradiation. *Journal of Saudi Chemical Society,* 19(5): 549-556.

Kołodziejczak-Radzimska, A. & Jesionowski, T. (2014). Zinc oxide—from synthesis to application: A review. Materials, 7(4): 2833-2881.

Kumar, K. V., Porkodi, K. & Rocha, F. (2008). Langmuir–Hinshelwood kinetics–a theoretical study. *Catalysis Communications,* 9(1): 82-84.

Kumar, M. P., Josephine, G. S., Tamilarasan, G., Sivasamy, A. & Sridevi, J. (2018). Rare Earth Doped Semiconductor Nanomaterials and its Photocatalytic and Antimicrobial Activities. *Journal of Environmental Chemical Engineering.* 6(4): 3907-3917.

Kumar, R., Umar, A., Kumar, G., Akhtar, M. S., Wang, Y. & Kim, S. H. (2015). Ce-doped ZnO nanoparticles for efficient photocatalytic degradation of direct red-23 dye. *Ceramics International,* 41(6): 7773-7782.

Mbule, P. S. (2009). Sol-gel synthesis of and luminescent properties of Pr^{3+} in different host matrices. Doctoral Dissertation, University of the Free State.

Phuruangrat, A., Yayapao, O., Thongtem, T. & Thongtem, S. (2014). Synthesis and characterization of europium-doped zinc oxide photocatalyst. *Journal of Nanomaterials,* 1-9.

Sakthivel, S., Neppolian, B., Shankar, M. V., Arabindoo, B., Palanichamy, M. & Murugesan, V. (2003). Solar photocatalytic degradation of azo dye: comparison of photocatalytic efficiency of ZnO and TiO_2. *Solar Energy Materials and Solar Cells,* 77(1): 65-82.

Sun, J., Qiao, L., Sun, S., & Wang, G. (2008). Photocatalytic degradation of Orange G on nitrogen-doped TiO_2 catalysts under visible light and sunlight irradiation. *Journal of Hazardous Materials,* 155(1): 312-319.

Varughese, G., Jithin, P. W. & Usha, K. T. (2015). Determination of optical band gap energy of wurtzite ZnO: Ce nanocrystallites. *Physical Science International Journal,* 5(2): 146.

Yi, F. & Chen, S. (2008). Effect of activated carbon fiber anode structure and electrolysis conditions on electrochemical degradation of dye wastewater. *Journal of Hazardous Materials,* 157(1): 79-87.

Zhuang, X., Wan, Y., Feng, C., Shen, Y. & Zhao, D. (2009). Highly efficient adsorption of bulky dye molecules in wastewater on ordered mesoporous carbons. *Chemistry of Materials,* 21(4): 706-716.